Deciphering sediment Connectivity Index and erosion pattern in a debris flow catchment

Loris Torresani, Vincenzo d'Agostino, Guillaume Piton

14th Congress INTERPRAEVENT 2021
Norway – Paper
www.interpraevent.at

Deciphering sediment Connectivity Index and erosion pattern in a debris flow catchment

Loris Torresani[1], Vincenzo D'Agostino[2], Guillaume Piton[3]

Keywords: Connectivity Index; protection measures; debris flow, GIS, hazard assessment, geomorphic analysis

Abstract

Understanding sediment connectivity and erosion pattern are fundamental in order to assess in a proper way actual and potential future hazard in debris flow prone areas. In this work, we propose a novel way to analyse and decipher the Connectivity Index (CI) applied in the Saint Antoine catchment, located in the French Alps. We conceptualised a procedure for the extraction of each variable involved in the CI computation along the thalweg profile. This new way to analyse CI helps to understand how this index is affected by past debris flow events and presence or absence of protection measures, also comparing protected reaches against non-protected reaches. This method opens new opportunity to use the Connectivity Index as an effective instrument to catch present or future hazard and support the planning of hazard mitigation measures.

Introduction

In Alpine regions, the occurrence of torrential processes is one of the major driving factors in morphology changes and sediment relocation as well as in threats endangering human assets. The availability of sediment and the capacity of a given stream to deliver it in areas at risk plays a leading role in the assessment of debris flow (DF) or debris flood risks. Thus, assessing sediment sources and sediment delivery processes is a crucial step to plan proper hazard mitigation measures.

However, this is a complex and challenging task, and it is specifically time-consuming at large scale, i.e., for catchments of 10-50 km². Many non-linear processes are involved in slope erosion and sediment transport (Ferro and Minacapilli, 1995; López-Vicente et al., 2015). Furthermore, anthropogenic activities are affecting sediment dynamics. Changing in flow paths related to roads and tracks on hillslopes, terraces, urbanisation over fan areas and agricultural expansion are examples of human impacts on the landscape with potential

[1] Dr., Department of Land, Environment, Agriculture and Forestry, University of Padova, Agripolis, Viale dell'Università 16, 35020, Legnaro (PD), Italy (loris.torresani@phd.unipd.it)
[2] Prof., Department of Land, Environment, Agriculture and Forestry, University of Padova, Agripolis, Viale dell'Università 16, 35020, Legnaro (PD), Italy
[3] Dr., Univ. Grenoble Alpes, INRAE, UR ETNA, 38000 Grenoble, France

complex side effects on geomorphology and hydrology. As a consequence, the change in landscape and land-use combined in some cases by climate changes, are accelerating the dynamics of slope erosion and degradation (Brown et al., 2016). This makes the task of geomorphic analysis even more challenging, and effects need to be addressed in order to have a complete perspective on sediment dynamics in a studied catchment.

To evaluate sediment dynamics, GIS-based indices have been developed since the 1970s (Atkinson, 1995; Dietrich and Dunne, 1978). Researchers have recently shown an increasing interest in studying the existing connection between sediment sources and channels.

The Connectivity Index (CI) is one morphometric index that for instance computes the existing degree of linkage between sediment sources (e.g. eroded areas on hillslopes) and sinks areas (outlet, hydrologic network, lakes). It was initially introduced in a work of Borselli et al. (2008) and then modified by Cavalli et al. (2013). Two concepts are the fundamentals of CI assessment: sediment delivery across the whole drainage system and sediment coupling/decoupling along the travel path from the source to the nearest sink. The CI is computed as the logarithm of the ratio between (i) an "upslope component", which is the product of square root of catchment area by mean slope by a mean value of upslope weighting factor; and (ii) a "downslope component" which is the sum of distance to downstream sink divided by the weighting factor and the slope of each pixel:

$$CI_k = \log_{10}\left(\frac{\overline{W_k}\,\overline{S_k}\,\sqrt{A_k}}{\sum_{i=k,\dots,n_k} {d_i}/{W_i S_i}}\right) \quad (1)$$

Where k is the pixel index for which the CI is computed, W_i is the weighting factor of pixel i and $\overline{W_k}$ is the mean value of W_i of all pixels located upstream of pixel k, S_i is the slope of pixel i and $\overline{S_k}$ is the mean value of S_i of all pixels located upstream of pixel k, A_k is the drainage area of pixel k, i.e., the contributing area; $k,\dots,n_k$ are the indexes of all pixels on the path from pixel k down to the target sink, and d_i is the path length in pixel i. The weighting factor (W) represents the impedance to sediment flows that can be based on different characteristics of the area. It can be computed from land use (using c-factors of the USLE-RUSLE model or Manning's n), or also from topography (Roughness Index).
The connectivity index (CI) varies in the interval [- ∞, + ∞]. In essence, CI increases with increasing sediment supply related to erosion rate proxy (weighting factor of upstream and downstream areas), upstream and downstream slope and catchment size, and decreases with distance to a downstream target.

Cavalli et al. (2013) adapted the CI to the alpine environment and to the use with high-resolution digital terrain models (HR-DTM) by introducing modifications that in essence (i) bounds to slopes in the range 0.5%-100% to focus on torrential flows and prevent bias-related to HR-DTM, (ii) uses the residual topography, i.e., standard deviation of the roughness height of the terrain as Weighting factor, to avoid using empirical parameters and because erosion processes tend to generate "noisy" topographies where flows are confined and thus transport more sediment and (iii) compute the contributing area with an algorithm that accommodates flow spreading on flat areas rather than artificially concentrating flow in one single lower pixel (D-infinity algorithm).

The CI computation, as described in Cavalli et al. (2013), is consequently fast and easy to use, requiring only an HR-DTM and the implementations of some GIS procedures. The same authors developed a specific GIS toolbox and a standalone application called SedInConnect that allows estimating the CI in a semi-automatic way (Crema and Cavalli, 2017).

Given this state of the art, there still exists a gap in this framework to be used in planning and designing hazard mitigation structures. In this context, a recent work by Cucchiaro et al. (2019) started to analyse the interaction of mitigation measures with CI but circumscribed to qualitative map interpretations. A quantitative interpretation of CI and changes provided by protection measures remain poorly unexplored.

This work seeks consequently to introduce a new quantitative way to analyse the CI, and highlights how the presence/absence of mitigation structures affects CI in the studied catchments. In general, we aim to apply for the first time this method and understand its potential to become an effective complementary tool for hazard assessment and mitigation measure planning in debris flow/flood-prone catchments. A French catchment, the Saint-Antoine torrent at Modane, is used as an application case after the occurrence in summer 2014 of a large DF event.

Assuming that check dams are mostly built to stabilise channel beds, while the open check dams aim at trapping debris flows, if CI analysis makes sense, we can hypothesise that (H1) connectivity index should be lower in the stabilised reaches than in the untrained reaches and (H2) that erosion rates should be lower where check dams are present, and deposition should obviously be concentrated in retention structures as open check dams.
CI is supposed to be lower on average with a regular drop of values in trained reaches. This because of the increased likelihood to flow diversion due to the new bed line (thalweg) induced by the presence of check dams. The component capturing this behaviour is the "upslope component" that encapsulates flow dispersion through the D-infinity algorithm used for drainage area computation. Also, the height drop at the check dam location will induce a certain degree of slope variation. The same attitude is expected to be visible from a DEM of Difference analysis (DoD) performed after the last DF event: more regular and moderate erosion rates are expected in reaches that are protected with check dams. Concerning non-protected domains in the Saint Antoine catchment, a consistently higher CI is expected due to the lower flow dispersion caused by higher flow confinement in the gorge. Besides, the channel is supposed to be more susceptible to randomly localised higher erosion or deposition rates.

In this work, the main stem of the Saint Antoine catchment (France) is studied. More precisely, the effects of the 2014 debris flow are analysed in the light of CI and of erosion/deposition assessment using LiDAR data taken before and after the event.

Methods

The Saint Antoine torrent is a tributary of the Arc River in the Western French Alps, located in the Community of Modane, Maurienne Valley. The drainage area of the catchment is 5.10 km^2, and ranges from 3065 m a.s.l. at Belle Plinier summit, to 1160 m a.s.l. at the outlet in the Arc River. The average slope is of 22%, and the Melton Index is 0.88. This catchment is prone to produce debris flow events; the oldest record dates back to 1489. In the last decades, two DF events occurred. One in 1987 with 55 000 m^3 to 80 000 m^3 of sediment deposited, and one in August 2014, with an estimated deposition of about 40 000 to 60 000 m^3. This catchment is characterised by the presence of 112 check dams and a unique open check dam located at the fan apex. The DTMs used in this work come from two different LiDAR surveys performed on 14th September 2010 and on 20th October 2014. As to the longitudinal analysis, the main channel was divided into five homogeneous domains (from A to E): (A) Upper trained reach, (B) untrained gorge, (C) trained gorge, (D) Open check dam, (E) Fan (Figure 1a).

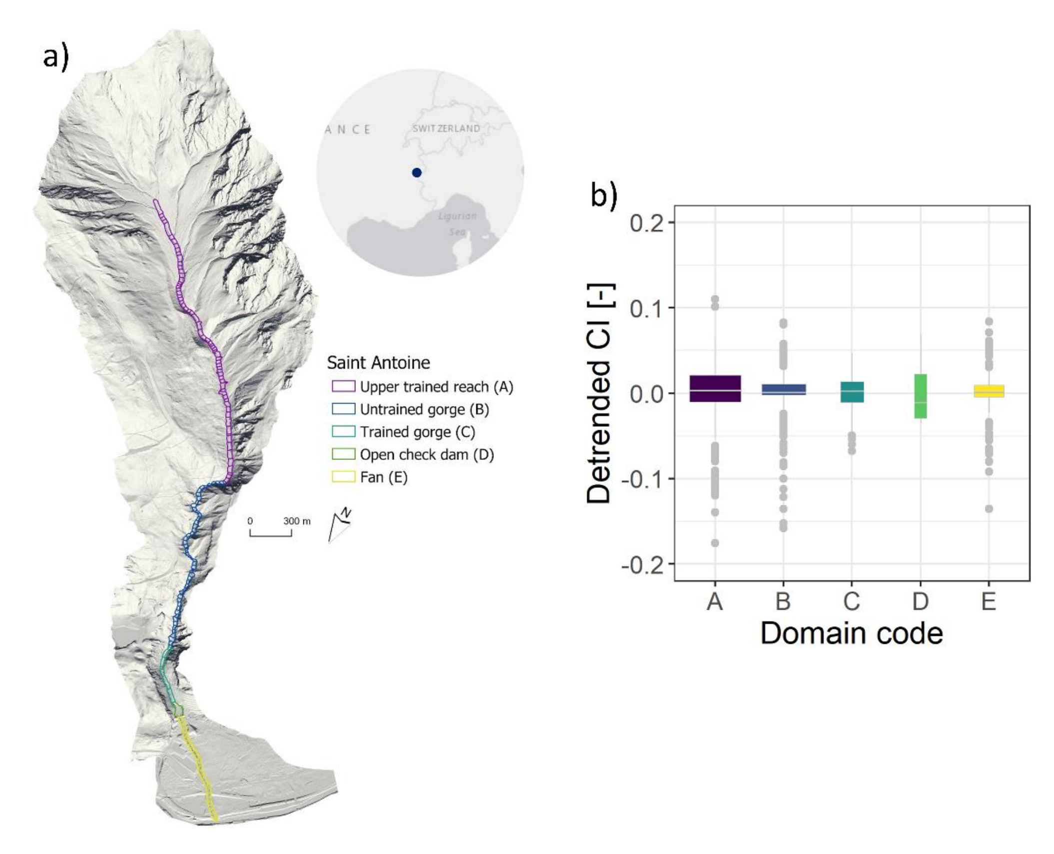

Figure 1. a) Map of the Saint Antoine catchment and alluvial fan and main domains: (A) upper main stem trained with more than 100 check dams, (B) intermediate reach, untrained, (C) lower main stem, trained by 5 check dams, (D) open check dam and (E) alluvial fan channel, embanked by dykes and b) boxplot of detrended connectivity index in the five main domains.

The method we propose is based on the longitudinal analysis of CI applied to a selected reach, e.g., the main channel or a tributary. The analysis was performed at two scales: at the pixel scale (5 m) for the extraction of CI, and at reach scale, i.e., integration on polygons that are as wide as the active channel and roughly 30 m long, i.e., same distance as between check dams. This resolution allowed to segment the channel bed in coherent units, i.e., reaches between check dams or reaches of equivalent length, for the extraction of erosion and deposition patterns and for comparison with reach-averaged CI values. The weighting factor (W) used in the CI computation was the topographic Roughness Index (RI). In particular, we choose to compute "W" on the 1m resolution DTM to highlight better Check-dam influence on surface roughness. This is achievable by the fact that the W computation is estimated by the standard deviation of residual topographic between the original DTM and a smoothed version over a 5 X 5 moving window. This results in a smoothing window size of 25 m^2 using the 1 m DTM, and 625 m^2 using the 5 m DTM. This aggregated W has then be used as a "Custom" Weighting factor in the second iteration of SedInConnect for the final estimation of the CI. There is a negative relationship between RI and CI: higher roughness corresponds to lower connectivity because terrain roughness affects sediment transfer capacity. It is worth stressing that extremely planar surfaces could invite flow spreading, resulting in reduced transport capacity, while rough surfaces could quickly develop confined flow paths with high transport capacity. However, this effect related to flow confinement is computed by the D-infinity algorithm and accounted for in the computation of the contributing area. For its use as Weighting factor, an inverse normalisation is needed to obtain values from zero (high RI) to one (low RI).

The first phase of the procedure is the production of the shapefile containing the sampling points needed for the longitudinal extraction of each variable composing the Connectivity Index. An easy way to obtain the point sampling layer was to convert a flow accumulation raster (using the D-8 algorithm) and filtered according to the drainage area of the reach under analysis, into a point shapefile. A quality check of this stream-line map was performed and proved to be a crucial step, which supported the choice to work with an aggregate 5 m pixel rather than the original 1 m pixel size. After that, the analysis was carried out on rasters with a pixel size of a coherent dimension with the investigated channel and process. This operation was necessary to reduce the micro-topography noise on the longitudinal analysis of CI and to focus only on the relevant geomorphic characteristics of a DF channel.

For the reach scale analysis, the integration with the(FluvialCorridor) toolbox presented in Roux et al. (2015) helped to extract riverscape features and aggregate them into homogeneous reaches using a semi-automatic procedure. The variables analysed at reach scale, mean and standard deviation values of CI, were derived from an aggregation of all cells within each reach.

The computation of the DEM of Differences (DoD) for sediment budgeting was obtained using multi-temporal DTM analysis derived from two LiDAR surveys. To improve results, a proper point cloud registration has been performed on assumed stable areas using the Iterative Closest Point (ICP) tool included in CloudCompare. This step was necessary to perform an accurate uncertainty estimation, and to filter noise and false-positive signals in elevation change.

An R script was produced for processing all the extracted variables and relate them with the geomorphic features of the investigated segments. Moreover, to better highlight check dam induced geomorphic variations over CI, an analysis of a linearly detrended CI was performed. This operation was based on removing the linear base trend (grey line on Figure 2) related to increasing catchment scale (on upslope component) and decreasing distance to the target (on downslope component).

Results and discussion

The first application of a longitudinal analysis on CI applied in Saint Antoine catchment allowed the understanding of the interaction between CI and the protection measures located along the main channel (Figure 1, 2).

The boxplot reported in Figure 1b displays the value of the detrended CI. It enables us to compare the variability of CI between each domain and the influence induced by the presence of hazard mitigation structures. We can see that CI varies markedly in the protected domains ("A" and "C"), i.e., boxplots have a wider interquartile range (IQR) than in the unprotected domains ("B" and "E").

Outliers are slightly wider in domain A than in domain B, mainly due to spreading near structure crest (Figure. 2e). Conversely, domains "B" and "E" (unprotected) show lower variability (lower IQR) in the CI value due to a more confined flow and the absence of protection measures. This is also visible in the detrended Upslope component on Figure 2e, is showing fewer drops and more stable stability in unprotected areas. This consistently higher connectivity should be considered more prone to transfer and to recruit sediment in the case of a DF due to the higher probability of the flow to incise or deposit material in this un-protected domain. Hence, we concluded refining hypothesis H1, that connectivity index is not specifically lower in the stabilised reaches than in the untrained reaches but clearly shows more varied distribution with low values in correspondence of consolidation structures and higher values far from check dams. In this work, we pushed further the CI analysis by understanding how it behaves quantitatively over different channel management conditions.

According to the CI analysis, erosion–deposition patterns displayed in Figure 2g are different for each specific domain. The protected domains "A" and "C" reported diffuse but regular values of erosions, generally lower than 1 m (as mean ± St. D, -0.43 m ± 0.24 m for domain A; -0.59 m ± 0.44 m for domain C), if compared with the non-protected domain B. Here reach-averaged erosion rate exceeded 2 m in some location but remained on average only slightly higher (-0.57 m ± 0.72 m). As to the domain "D" of the open check dam, is the domain with the highest deposition rate (1.83 m). In domain "E", the fan channel experienced low erosion rates in the upper part, followed by some sediment depositions near the outlet with the Arc River; this is consistent with the usual behaviour of debris flows on fans. Our working hypothesis H2 is here validated since erosion rates are lower where check dams are located, and deposition is concentrated in the open check dam. It is worth stressing that the trends on domains "A" and "B" are however extremely oriented toward erosion caused by the August 2014 DF. Conversely, reports from ONF RTM archive relates major deposition in the downstream part of domain "A" during the event of 1987 and let presume that basin behaviour is massively variable.

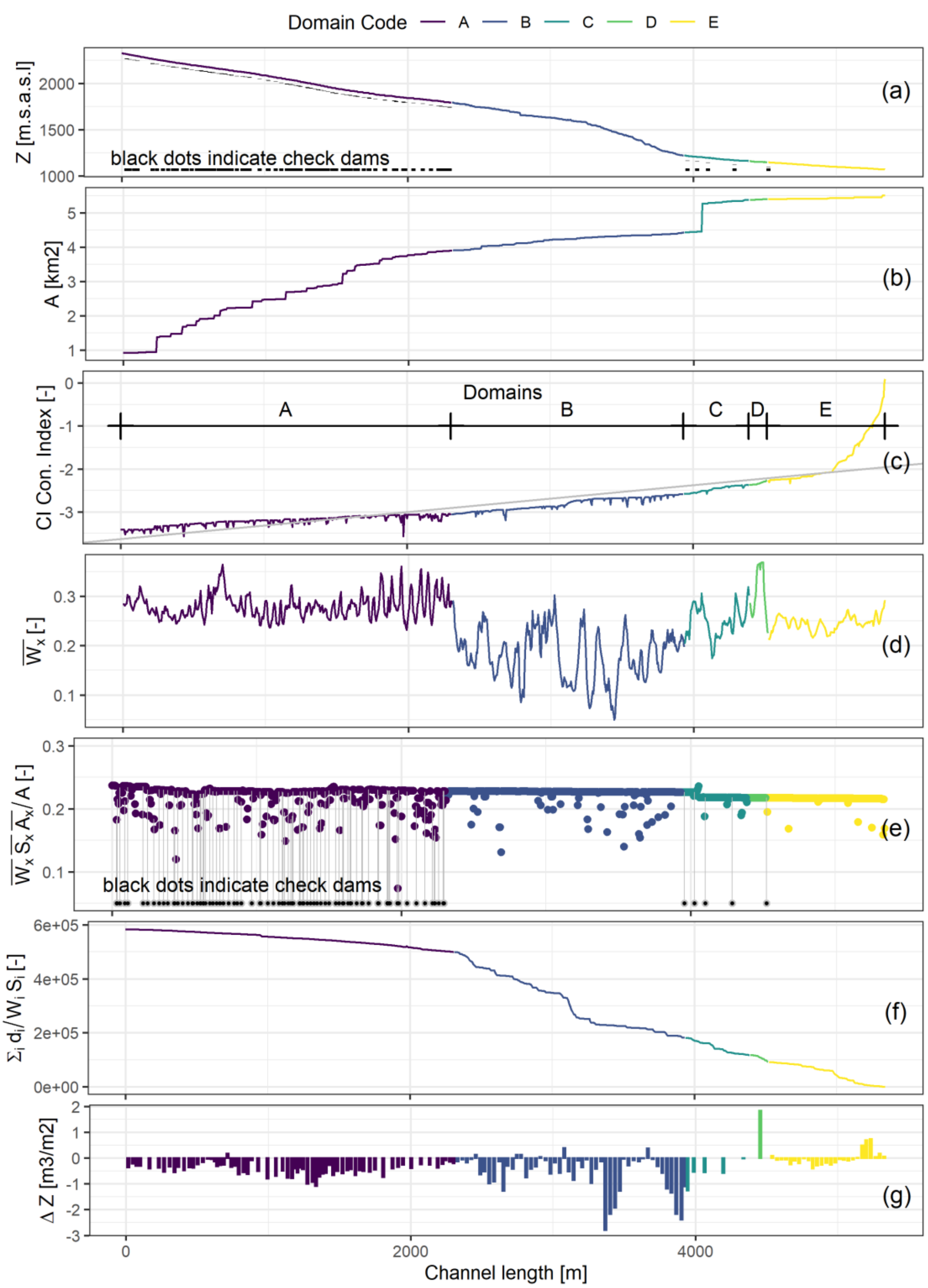

Figure 2. Longitudinal analysis of the Saint Antoine main stem according to our procedure: a) longitudinal profile highlighting the domain and location of check dams, b) upstream catchment area, c) connectivity index, d) Weighting factor, e) detrended upslope component, i.e., upslope component divided by square root of contributing area, f) downslope component and g) erosion and deposition rate (m3/m²) aggregated at reach length (30 m long) from DoD

The catchment size increases gradually (Figure 2b) as well as the CI (Figure 2c) except for a fast increase in the more distal part of the fan where the downslope component drops to zero (Figure 2f), and thus CI increases markedly. The drop in the downslope component is mainly related to the regular decrease in distance since the weighting factor oscillates between 0.15 and 0.6 (Figure 2d). Regarding the weighting factor, in domain “A” is fluctuating rhythmically between 0.3 and 0.6. The lower point of each swaying cycle falls in the area where a Check Dam is located.   In domain B (un-trained) the weighting factor varies greatlyinside the range 0.15 to 0.6, but with a lower mean value . The weighting factor variable explains a moderately higher roughness in domain B, which can be explained by the higher confinement of flow and higher irregularities in the topography induced by a gorge morphology.

The upslope component detrended by the square root of the contributing area is rather stable except for local drops that are more numerous in domain “A” than in other downstream domains (Figure 2e). Visual inspection of the maps demonstrated that flow spreading on the reaches located directly upstream of check dams is responsible for these drops.

In a global perspective of Figure 2, the relation between elevation changes and all the other variables appear interesting. In particular, it is possible to see how each variable has different patterns according to the analysed domain.

Conclusion

From the results, we can conclude that this first quantitative analysis of CI along the main channel opens new opportunities for the interpretation and use of the Connectivity Index as a tool for geomorphic features analysis of a selected catchment. It also enables us to understand how each factor encapsulated in the CI framework is affected by the long-term presence of protection structures. Moreover, we observed that some interesting correspondence appears between different statistical distributions of CI and geomorphic changes in case of a debris-flow event. Advanced analyses on the previous point are ongoing extending the application of this novel method to tributaries. This will help to test the global versatility of the approach on heterogeneous mountain catchments.

Through this new procedure, we are opening a new way to analyse the connectivity index and its possible use during hazard mitigation planning and hazard assessment. In particular, after further applications, we might deliver an easy-to-use procedure for CI interpretation that can be used to understand sediment dynamics in mountain torrents.

Acknowledgement

The authors would like to thanks the ONF RTM for providing data on the torrent. The work of G.P. was funded by the H2020 NAIAD project [grant no. 730497] from the European Union’s Horizon 2020 research and innovation program.

References

Atkinson, E., 1995. Hydrological Sciences Journal Methods for assessing sediment delivery in river systems. Hydrol. Sci. J. 4040, 273–280. DOI:10.1080/02626669509491409

Borselli, L., Cassi, P., Torri, D., 2008. Prolegomena to sediment and flow connectivity in the landscape: A GIS and field numerical assessment. Catena 75, 268–277. DOI:10.1016/j.catena.2008.07.006

Brown, A.G., Tooth, S., Bullard, J.E., Thomas, D.S.G., Chiverrell, R.C., Plater, A.J., Murton, J., Thorndycraft, V.R., Tarolli, P., Rose, J., Wainwright, J., Downs, P., Aalto, R., 2016. The geomorphology of the Anthropocene: emergence, status and implications. Earth Surf. Process. Landforms. DOI:10.1002/esp.3943

Cavalli, M., Trevisani, S., Comiti, F., Marchi, L., 2013. Geomorphometric assessment of spatial sediment connectivity in small Alpine catchments. Geomorphology 188, 31–41. DOI:10.1016/j.geomorph.2012.05.007

Crema, S., Cavalli, M., 2017. SedInConnect: A stand-alone, free and open-source tool for the assessment of sediment connectivity. Comput. Geosci. DOI:10.1016/j.cageo.2017.10.009

Cucchiaro, S., Cavalli, M., Vericat, D., Crema, S., Llena, M., Beinat, A., Marchi, L., Cazorzi, F., 2019. Geomorphic effectiveness of check dams in a debris-flow catchment using multi-temporal topographic surveys. Catena 174, 73–83. DOI:10.1016/J.CATENA.2018.11.004

Dietrich, W.E., Dunne, T., 1978. Sediment budget for a small catchment in mountainous terrain. Z. Geomorph. N. F., Suppl. Bd. 29, 191–206.

Ferro, V., Minacapilli, M., 1995. Sediment delivery processes at basin scale. Hydrol. Sci. J. 40, 703–717. DOI:10.1080/02626669509491460

López-Vicente, M., Quijano, L., Palazón, L., Gaspar, L., Navas, A., 2015. Assessment of soil redistribution at catchment scale by coupling a soil erosion model and a sediment connectivity index (central spanish pre-pyrenees). Cuad. Investig. Geográfica 41, 127. DOI:10.18172/cig.2649

Roux, C., Alber, A., Bertrand, M., Vaudor, L., Piégay, H., 2015. “FluvialCorridor”: A new ArcGIS toolbox package for multiscale riverscape exploration. Geomorphology 242, 29–37. DOI:10.1016/j.geomorph.2014.04.018